Hydrogeology Journal (2023) 31:1353–1370
https://doi.org/10.1007/s10040-023-02635-4

TECHNICAL NOTE

# How to conduct variable-density sand tank experiments: practical hints and tips

L Stoeckl[1] · G Houben[1]

Received: 28 July 2022 / Accepted: 29 March 2023 / Published online: 10 May 2023


**Abstract**
Sand tank experiments are a powerful tool for the investigation and visualization of groundwater flow dynamics. Especially when studying coastal aquifers, where the presence of both fresh and saline water induces complex variable-density flow and transport processes, the controlled laboratory settings of tank experiments help scientists to identify general patterns and features. This technical note provides practical information on planning, conducting and evaluating sand tank experiments, with a focus on application to coastal hydrogeology. Materials, e.g. the sand tank itself, liquids and porous media, are discussed, as well as their handling and auxiliary equipment. The collation of hints and tips is intended to guide novices, as well as experienced researchers, and possibly prevent them from repeating the errors that have been encountered during a long history of experimental work conducted by the authors and researchers associated with many other published studies.

**Key words** Laboratory experiments/measurements · Salt-water/fresh-water relations · Coastal aquifers · Groundwater density/viscosity · Groundwater flow

## Introduction: What are sand tank experiments and what can they be used for?

Sand tank experiments with a focus on coastal hydrology (density-dependent flow) have a long history and go back to the early 20th century. One of the first known experiments was performed by Pennink (1905), who visualized groundwater flow paths in a coastal aquifer set-up and performed pumping experiments in a two-dimensional (2D) sand tank. Instead of saltwater, he used milk, which was denser and could easily be distinguished from freshwater. Even though photographs were taken, hydrochloric acid added to the water was used to etch flow paths into a zink plate at the back of the tank for subsequent interpretations.

Since these early, more general experiments, plenty of designs and techniques have evolved to investigate flow and transport in coastal aquifers in sand tanks. Experimental applications cover a wide spectrum of applications, e.g. reactive tracers (Abarca and Clement 2009) and chemical reactions (Panteleit et al. 2011), multi-tracer experiments (Stoeckl and Houben 2012), unsaturated (Thorenz et al. 2002) and transient flow conditions (Röper et al. 2015), geotechnical engineering (Luyun et al. 2011), including three-dimensional (3D) experiments (Oswald et al. 2002) for the benchmarking of numerical model codes. This technical note serves as guide for novices and experienced scientists on how to build a sand tank, providing information on planning, conducting, and visualization, focusing on variable-density flow and transport in coastal environments. Recommendations on the materials, the auxiliary equipment, and their handling before, during, and after an experiment, stem from a long history of experimental work by the authors and many other published studies. Valuable information on what "to do" and "not to do", hints and workarounds may help scientists to more easily and reliably plan and set up their experiments.

## The sand tank

### General typology

The focus of this article is on classical sand tank experiments at the macro-scale, using porous media as aquifer material equivalent. Such 2D set-ups are the most commonly

✉ L Stoeckl
Leonard.stoeckl@bgr.de

[1] Bundesanstalt für Geowissenschaften und Rohstofffe, Stilleweg 2, 30655 Hannover, Germany

used experimental types of sand tank experiments. They consist of a tank, usually rectangular, representing a cross-section through a coastal aquifer and adjacent features, e.g. the ocean, rivers or reservoirs. Other types and geometries are also possible but will be discussed only briefly in the following:

Probably the simplest sand tank design is a column filled with sand (or other porous media), simulating one-dimensional (1D) flow. Such column experiments are usually carried out to study transport processes, e.g. tracer or chemical reactions. These may be stand-alone experiments (e.g. Boluda-Botella et al. 2008; Nomitsu et al. 1929; Zhou et al. 2009), or used as prerequisites for 2D or 3D experiments, by determining relevant parameters, such as hydraulic conductivity and dispersivity of a porous medium (Cahill 1973), or propagation rates of a certain dye (Zhang et al. 2002). Column experiments may be set up either horizontally, or more commonly vertically, when combined with variable-density flow. Tides may be simulated in 2D experiments as well, by pumping saltwater in and out at the bottom of a saltwater saturated column with freshwater above (Pool et al. 2016).

Hele-Shaw experiments can be seen as predecessors or alternatives to classical sand tank experiments. In the absence of a porous medium, fluid flow is observed between two translucent plates with a very narrow spacing ranging from 0.2 to 1.65 mm (Anwar 1983; Wooding et al. 1997). Density-driven flow may be simulated by employing two or more phases (Bear and Dagan 1963). However, the absence of a porous matrix imposes several restrictions, e.g. geological heterogeneity or different hydraulic conductivities cannot be simulated. Examples of Hele-Shaw experiments for coastal groundwater include Anwar (1983), who investigated the effect of subsurface barriers on saltwater intrusion (SWI), Wooding et al. (1997), who developed a physical benchmark of an evaporating salt lake, and Cooper et al. (2000), who visualized double-diffusive finger convection. A detailed review of Hele-Shaw models, however, is not the objective of this article. Additionally, microfluidic experiments, which study processes on a (sub)millimeter scale have also been done to observe the interaction of fluid phases of different densities (e.g. Borgman et al. 2019).

## Geometries and dimensions

The length of a sand tank varies from several centimeters to over 10 m, with a spacing of usually a few centimeters to up to 1 m in between the front and the rear wall (Robinson et al. 2015; Yu et al. 2019). This aperture of the sand tank implies that the porous material installed therein is not a 2D body in the strict sense. However, effects of 3D flow are often ignored. As the porous medium is normally backfilled from above, a model should not be much higher than around 1.5 m to ensure proper handling (Abdollahi-Nasab et al. 2010; Werner et al. 2009).

Fully 3D set-ups are more realistic when considering, e.g. seawater up-coning by pumping, or groundwater flow in circular islands. They are, however, less common, as they are more difficult to handle and observe. Larger volumes of sand, water and tracer are usually required, resulting in elevated loads acting on the wall and the floor. Direct (visual) observations and measurements can be conducted only at the boundaries of a transparent tank—what is happening within remains invisible. Indirect, geophysical measurement methods (described in section 'Automated image processing') may help to measure processes in such 3D experiments (Pearl et al. 1993). Wedge-shaped (pie slice) sand tanks were commonly used to study radial freshwater flow, e.g. radially symmetric flow towards a well; however, they can also be used for density-driven flow, e.g. for up-coning studies around a pumping well. Memari et al. (2020) used such a set-up to study the flow of fresh and saline water in a 15° segment of a circular island. Sizes of 3D set-ups may vary from several cubic centimeters, e.g. when being placed into a geophysical observation facility (Pearl et al. 1993), to up to over 1 $m^3$ when, e.g. external geophysical measurement techniques, are applied.

## Sand tank materials

The walls of a sand tank are commonly constructed using transparent materials, allowing the visual observation of flow with the help of tracer dyes. In some cases, e.g. 2D column experiments, nontransparent materials may be used when parameters are measured in the outflow water only, e.g. the breakthrough of a salt tracer by electrical conductivity. The classical material for constructing sand tanks has been glass, which is sometimes still being used (e.g. Jazayeri et al. 2021; Kuan et al. 2012; Werner et al. 2009); however, the majority of models nowadays are made of acrylic-glass (e.g. Faulkner et al. 2009; Goswami and Clement 2007; Röper et al. 2015; Stoeckl et al. 2015; Wu et al. 2019), as it is ~40–50% lighter than glass, more flexible, and has a higher impact strength. Unlike glass, it also allows for easy modifications after construction, e.g. the drilling of additional sampling ports. One downside is that thermal ultra violet (UV) radiation of water with different temperatures is more dampened in acrylic-glass compared to glass, inhibiting thermal imaging.

The thickness of the sand tank walls depends on the pressure exerted by the backfill material and the water in the pores (and on the material chosen). The resulting buckling pressure should be calculated before designing the sand tank, using the classical geotechnical equations. Additional small fixtures at the top between the front and rear wall contribute to the overall stability of a model (see Fig. 1). This can be

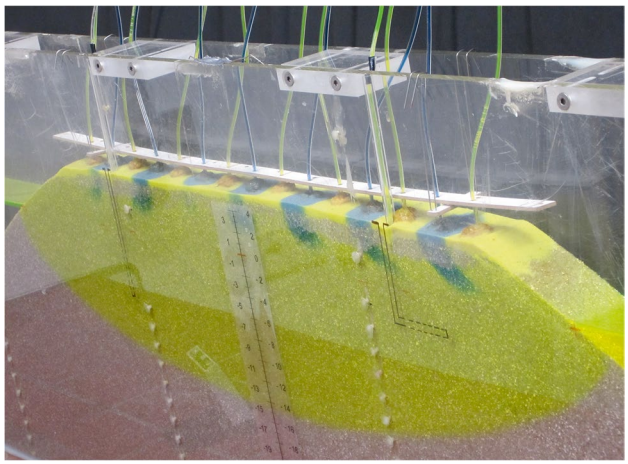

**Fig. 1** Single row of drippers in wooden holder above the island providing recharge (alternating blue and yellow) to a freshwater lens (yellow) floating on top of saltwater (light red). The drawing on the tank surface indicates the position of a horizontal well. Also note the vertical scale installed in the middle used to measure the freshwater thickness (here 15 cm below sea level) over time and the vertical rows of injection/extraction ports sealed with white silicone (set-up as used in Stoeckl and Houben 2012)

crucial to prevent a tank from bulging in the middle, thus ensuring a consistent spacing. For very large experimental tanks, additional bars or braces on the outside have to be added for stability. For standard sizes, e.g. smaller than 2 m × 1 m, acrylic-glass wall thicknesses between 0.6 and 1.5 cm are common (Sharma and Bhattacharjya 2020; Werner et al. 2009).

## Auxiliary measurement equipment

Depending on the set-up of the model and the research question, certain auxiliary measurement equipment has to be used. Although the reader is encouraged to look out for new developments and inventions, some details on well-established and useful standard equipment are given here.

In coastal hydrogeological laboratory experiments, the most important parameters of interest are commonly the hydraulic head and solute concentrations. Head distributions determine hydraulic gradients and influence the salinity distribution, and vice versa. A simple mm-scale, printed on transparent paper can be attached to the tank to track interface levels and the thickness of freshwater lenses (Fig. 1). The height of a supply tank or a Mariotte's bottle above the base level should be measured for determining the water level. Head measurements in the tank are, however, disturbed by the capillary rise in the porous media. Mini-piezometers (observation wells) can be installed, preferably through perforations at the back wall, which prevents flow disturbances and obstruction of the view (e.g. Morgan et al. 2013). They are vertical translucent pipes, which allow the observation of the water level within. Multiple piezometers installed in different locations form a piezometer "organ", "harp" or "board" (Rumer and Harleman 1963). Water volumes in the piezometers should be accounted for, when planning the use of multiple piezometers, as head changes in the tank may lead to considerable water gain or loss by piezometers. Piezometer diameters should thus not be too large to store large quantities of water, neither too small to be susceptible for capillary rise effects within. Reference values are between 0.5 cm and max. 1 cm, depending on the material (e.g. glass or pvc) and shape (round tubes or squared columns). A proper communication with the experimental chamber must be ensured by preventing the piezometers from clogging, e.g. by the use of a mesh at the in-/outlet.

The hydraulic head may also be measured as water pressure by the use of mini-pressure transducers installed at the bottom of the tank (Wu et al. 2019). Such devices have the advantage of recording data continuously and automatically or in defined intervals, when connected to a logger or PC. Similarly, salinity or total dissolved solids can be measured automatically by installing electrical conductivity mini-probes from the rear of a sand tank (Oz et al. 2016). A high spatial resolution is, of course, desirable, but many electrodes may obstruct the flow within the tank. Larger, commercial hand-held probes can be used to measure physico-chemical parameters outside the tank, e.g. pH, salinity and temperature for the calculation of water densities of in- and outflow waters. Flow velocities are usually not measured directly in sand tank experiments, even though applications of the magnetic induction or the ultrasonic sound method may be possible. For the analysis of flow velocities and directions, the movement of tracer dyes is usually observed and a calibrated numerical model may additionally be helpful.

Sampling ports in the tank walls can be installed by drilling (Fig. 1). Their number and position can be adapted to the research question. It is advantageous to have them all on one side of the tank, usually the back side, to provide a clear field of view for photography/filming on the other side. Threaded holes can be closed by threaded plugs. Unthreaded holes can be sealed with silicone, which allows for manual sampling and injection of small amounts of (tracer) water using a syringe needle, since the silicone will self-seal the needle hole.

Wells that extract water from the sand tank can be emulated in different ways, such as by use of a needle (Abdelgawad et al. 2018), or water can also be extracted from sampling ports with valves, allowing for, e.g. continuous sampling and hydro-chemical analysis in the case of chemical reaction experiments. These two methods, however, may induce 3D flow towards the single extraction point. For 2D cross-sectional models, a physical mini-model of a well, i.e. a perforated pipe can be installed, with the

perforated section emulating the well screen. The well has to be sealed at the screen end and connected to a tube and pump at the other (Jakovovic et al. 2011; Shi et al. 2011; Stoeckl et al. 2019; Vats et al. 2020). Its location (length and height) can easily be modified. Stoeckl and Houben (2012) installed both vertical and horizontal well screens to test their influence on saltwater up-coning. It should be noted that the drawdown around these mini-wells is affected by the proximity of the sand tank walls, which act as impermeable boundaries. Therefore, a more 2D representation of a well, however less flexible, can be achieved by a perforated tube which fully covers the sand tank aperture between the front and the rear wall. This minimizes 3D effects, because water is then extracted over the whole screen length. In 3D cube models, pumping can either be represented in the middle of a sand tank wall using a mini-well or from one corner, simulating a quarter of a radial well. Radial (pie) slice models are the most efficient to study flow towards a well, since the radial acceleration of the flow velocity is prescribed by the geometry.

Water supply tanks are necessary for mixing and storage of water used for the equilibration period and during the experiment. Tanks should be large enough to provide a sufficient volume of water, yet small enough to handle degassing; in general, storage tanks or (glass) bottles of around 50 L are a good choice.

Placing a clock or stopwatch in front of the sand tank is recommended so that the time will always be visible in the later evaluation of photographs and films. The time is needed to keep track of the movement of tracer dyes and the interface over time, or of changes in the boundary conditions applied at certain times or intervals. Tools for optical measurements are described in section 'Visualization using tracer dyes'.

Tides have a crucial influence on coastal hydrogeology and have been studied extensively in sand tank experiments (e.g. Fang et al. 2021; Kuan et al. 2019; Pool et al. 2016; Röper et al. 2015; Shen et al. 2020). They can be generated by manipulating the saltwater level in the "ocean" reservoir, which is usually done by inserting and retracting a suspended displacement body (slug, plunger) in a sinusoidal pattern over time. This is best done automatically by a programmable apparatus; and in the ideal case, even the influence of neap and spring tides can be emulated. Complex tidal signal may also be achieved by, e.g. a bidirectional water pump, pumping water in/out a reservoir into/out of the experimental chamber, respectively (Wu and Zhuang 2010).

Pumping-induced ground movement (land subsidence) can also be studied in sand tanks. Laboratory experiments conducted by Zhang et al. (2022) investigate the development of earth fissures caused by the deformation of a clay layer due to pumping. They measured horizontal and vertical ground displacement, using laser rangefinders on the surface of the sand and displacement transducers, respectively.

## Porous material characteristics and backfilling techniques

A wide range of materials is available as matrix material for sand tank experiments. The use of natural sediments is rare (e.g. Lu et al. 2013), as it is difficult to obtain a representative and repeatable sample. Sampling in the field and backfilling into the sand tank will also destroy the natural texture and degree of compaction. The often-opaque grains make discerning color tracers added to the pore fluid difficult and some minor constituents may lead to unwanted reactions in the sand tank (e.g. swell-able clays, carbonates, organic matter, iron oxides). For the sake of control in a laboratory model, it is also preferred to exactly know the hydraulic properties of the material used. Homogeneity is important when trying to understand certain processes which might be disturbed by heterogeneous samples collected from nature or by uneven backfilling. Oliviera et al. (1996) describe different packing techniques for sand column experiments and report that denser and more uniform packing was achieved by wet packing and by vibrating the column.

Many authors therefore use glass beads instead (e.g. Abdelgawad et al. 2018; Abdoulhalik et al. 2017; Etsias et al. 2020; Robinson et al. 2016, 2015). They are commercially available, at reasonable prices, in standardized grain size classes, each with narrow particle size distributions (e.g. 1.0–1.3, 1.25–1.65, 1.7–2.1, 2.0–2.4 mm). The high sphericity of the grains and their well-defined uniform particle size provide a highly idealized surrogate sediment with good permeability and high pore volume. Due to their transparency and lower degree of light refraction, they allow a better tracking of color tracers in the pore fluid, e.g. when using automated image tracking (e.g. Robinson et al. 2016, 2015). Another advantage is the lower adsorption of color tracers compared to quartz sand. A problem with fine-grained dry glass beads is their electrostatic charging which, according to the authors' experience, occurs at grain sizes smaller than 2 mm. They thus tend to stick quite tenaciously to any charged surface, including the sand tank, and are difficult to remove. When spilled on the floor, glass beads constitute a significant slip hazard.

Filtering glass is cracked glass with irregular grain shape and was used by Engelmann et al. (2019) for dense non-aqueous phase liquid (DNAPL) migration and entrapment studies. It represents natural nonconsolidated porous media well and is thus a promising alternative to cost-intensive spherical glass beads.

A good compromise is the use of well-sorted filter sands (e.g. Dose et al. 2014; Houben et al. 2018; Shen et al. 2020; Stoeckl and Houben 2012). Such sands (and gravels) are

readily available as bulk commercial products, as they are used in water treatment and well construction. Compared to glass beads, they are cheaper and closer to actual sediments regarding grain and pore shape, and they are obtained from natural, quartz-rich sands by wet sieving, which removes clay and silt particles, and tumble washing, which removes most of the coatings from the quartz grains. They are available in several standardized grain size classes, ranging from fine sand (0.4–0.8 mm) to very coarse sand (1.6–2.5 mm) and even gravel. The chemical composition is also standardized with the $SiO_2$ content usually being higher than 96 wt.% $SiO_2$. The almost exclusive predominance of quartz is important, as higher contents of, e.g. feldspar and calcite, can lead to the secondary formation of fine grains, e.g. during backfilling, since both minerals have a distinct cleavage and fracture easily. Reproducibility is assured through standards, e.g. European Norm EN12904 (2005).

Mathematical modeling of sand tank experiments requires knowledge of the hydraulic conductivity and the porosity of the materials. There are several ex-situ methods to do this, e.g. based on grain size analysis (e.g. the well-known Hazen and Kozeny-Carman equations) or Darcy permeameter tests. They have the general disadvantage that the degree of compaction of the studied material and that of the material backfilled into the sand tank may differ significantly, which will influence both porosity and conductivity. For homogeneous sand tanks, it is therefore recommended to measure these parameters in-situ, i.e. in the backfilled sand tank. For the porosity, this is fairly easy: the volume of water required to fully saturate the material in the sand tank is recorded. Measuring the volume drained from a saturated tank is also possible; however, losses by water retained in the capillary fringe have to be considered. The hydraulic conductivity can be obtained from a steady-state Darcy test adapted to the rectangular geometry, using an equation proposed by Forchheimer (1914):

$$K = \frac{2LQ}{b(H+h)(H-h)} \tag{1}$$

where

$K$ = hydraulic conductivity [L/T]
$Q$ = flow rate [$L^3$/T]
$L$ = length of sand tank (distance between water reservoirs) [L]
$H$ = water level at inflow side [L]
$h$ = water level at outflow side [L]
$b$ = breadth (aperture) of the sand tank [L]

In nonhomogeneous, e.g. layered tanks, this test will return the overall hydraulic conductivity of the backfill materials. Pumping tests, using wells installed in a sand tank, are generally not recommended because the sand tank walls will act as impermeable boundaries and will thus prevent the application of classical analytical models for pumping test interpretation. However, in 3D tanks, pumping tests are possible, provided that the cone of depression does not reach the boundaries.

The aquifer grains will always obstruct the visualization of processes in the pore fluid due to their opacity and the scattering and refraction of light. Choosing a solid material with a refractive index close to that of the fluid would make the solid visually "disappear" from the image (Iskander 2010). Hydrogel, a water-containing polymer, which can be obtained as spheres, fulfils this requirement to a high degree. The approach was applied by de Vriendt (2021) in order to better visualize chemiluminescent mixing reactions in porous material. Hydrogel beads, however, have the undesirable tendency to swell and disintegrate when exposed to water for a longer time, especially under saline conditions. Fluorinated ethylene propylene (FEP) grains should have promising optical properties but commercially available material is often disappointingly opaque. Nafion, a sulfonated tetrafluoroethylene-based fluoropolymer-copolymer also has promising properties but is extremely expensive (de Vriendt 2021). Another approach is to chemically modify the refractive index of the pore fluid to make it match that of the matrix grains, e.g. by adding glycerol. This, however, leads to modifications of the fluid density and viscosity, which is undesirable in experiments of density-dependent flow.

Impermeable layers can be simulated by ductile material such as silicone, natural or modelling clay (e.g. bentonite), or plasticine (Abdoulhalik et al. 2017; Houben et al. 2018; Pollock and Cirpka 2012), of which the latter is flexible, cheap, readily available (e.g. from toyshops) and comes in different colors. Gypsum plaster can also be used, however, mostly for models where the backfill remains in place for longer times, e.g. in models used for educational purposes. Impermeable walls can also be simulated by inserting strips of solid material, e.g. plastic (Armanuos et al. 2019; Luyun et al. 2011; Shen et al. 2020).

Water-soluble backfill material can be used to study dissolution by flowing groundwater, e.g. for subrosion and land subsidence studies. Oz et al. (2016) used consolidated halite blocks from recent salt deposits along the shore of the Dead Sea (Middle East) to simulate dissolution processes and sinkhole formations, and Moore et al. (2021) used salt cores from a Canadian evaporate formation.

Features of high hydraulic conductivity, such as fractures (or caves) can be emulated by stainless steel mesh screens molded around a steel rod, resulting in hollow mesh cylinders, as done by (Etsias et al. 2020). In experiments of coastal groundwater flow, the slope of the beach face is often varied to study the impacts of tides and storm inundations (Röper et al. 2015). All the materials discussed in the

preceding have a natural angle of repose, which limits the maximum slope possible. Higher angles can, however, be attained by stabilizing the slope by a meshed band.

Granular materials should be homogenized prior to backfilling, since segregation of grain sizes may occur in the bag during transport. Washing is also recommended, in order to remove dust. Even for commercial, standardized material, a particle size analysis is always recommended to verify the grain sizes. All sand tank aquifer materials, including glass beads, can be installed at different rates of compaction (or bulk densities). The mass of the installed material should therefore always be measured and divided by the occupied volume of the sand tank to ensure reproducibility. Compaction can be attained by tapping onto the sand tank or vibration, e.g. using a mobile ultrasonic source. The material should be installed layer-wise under water-saturated conditions to minimize the entrapment of air bubbles, which otherwise reduce the permeability; therefore, the water table should be raised step-wise with each layer. At the end, the model should be flushed with at least one or two pore volumes of degassed water to displace entrapped air and dust. Simple dumping of large volumes of aquifer material in one step may lead to grain size segregation. When lateral variations of materials are required, backfilling of the individual compartments is best done between two flexible rulers (e.g. Houben et al. 2018). Removal of aquifer material from the sand tank after the experiment can be done in the wet, fluidized state, using an industrial vacuum cleaner, whereas material from smaller sand tanks can be dumped or flushed out with a hose.

## Fluids

### Input water conditions

The most common fluid used in sand tank experiments is tap water, since it is cheap and available in almost any desired quantity. It should, however, be inert as much as possible from a chemical point of view, in order to prevent both chemical attacks on the sand tank materials and clogging. If the water supply company cannot provide details, a hydro-chemical analysis of the water is recommended prior to the experiment. In most countries, tap water has a circumneutral pH and contains no aggressive dissolved carbon dioxide, thus preventing the dissolution of carbonates, which can be present in sand material. Concentrations of dissolved iron and manganese should be very low in order to prevent precipitation, clogging and staining. Using tap waters of elevated hardness (both carbonate and sulphate hardness) is discouraged, since it tends to deposit carbonates or sulphate scale during the experiments. They can form a whitish film on surfaces, affecting the translucence of the (acrylic-) glass and are quite tedious to remove. Such waters should be diluted with or replaced by distilled water. Previous boiling of the water will also reduce later precipitation.

Generally, water has to be degassed prior to use, preventing air bubble entrapment in sediment pores. Entrapped air inhibits flow and diminishes the hydraulic conductivity. Degassing can be achieved by boiling, while ultra-sonic treatment is another option; however, due to the generally small volumes treatable (e.g. around 5 L), it has to be performed over a long period of time. To the authors' knowledge, the best method is a hydrojet-vacuum pump connected to a large (e.g. 50 L) glass bottle, which can additionally be placed on a magnetic stirrer to accelerate degassing (Fig. 2; Stoeckl and Houben 2012). Stirring also aids in dissolving salts and tracer dyes.

Tap water also forms the basis for artificial seawater, since actual ocean water is often difficult to obtain and to handle, as it requires transport to the laboratory and filtration to remove suspended fines and organisms that otherwise can lead to clogging and biofouling. Table salt is commonly used for this purpose, as it is cheap and readily available; although, it should be noted, however, that commercially sold salts often contain additives (up to 10 g/kg),

**Fig. 2** Degassing of water via vacuum in a 50-L glass container using a water-jet pump (not shown) and a magnetic stirrer below the container, which aids in the expulsion of the gas bubbles

which prevent agglutination to keep the product flowable. While preparing a saltwater solution, these poorly soluble additives accumulate as sludge at the bottom of the bottle, which should be separated and discarded.

The density of saltwater can be measured using different techniques. The easiest way is weighing the water contained in a vessel of defined volume. Hydrometers (areometers) using the Archimedes principle are also common, and usually consist of a closed hollow glass tube, where ballast material, e.g. lead beads, are placed into a wider bottom part, above which a narrow graduated stem is located. The water to be tested is filled into a graduated cylinder, into which the hydrometer is then gently lowered until it floats freely, without moving. The density is then read off from markings on the graduated stem, i.e. where the water surface touches it. Pycnometers are another option. If nonstandard temperatures prevail in the lab, corrections have to be made. More exact readings can be done by digital density meters, which are very accurate but expensive instruments. Several other measurement principles are in use, including hydrostatic pressure, float buoyancy, ultrasonic, refraction, vibration and even radioactive radiation. The authors have had good experiences with vibrating element transducers: a U-shaped tube is filled with the sampling liquid and brought to vibration. Determining the resonant vibrational frequency allows for determining the density. In any case, it is strongly recommended to measure, and not only calculate, water densities when using different liquids in an experiment.

For experiments investigating the oil–water interface, an important topic both in petroleum reservoir and groundwater contamination studies (Jung et al. 2006; Pokrajac and Deletic 2006), water is replaced by nonaqueous phase liquids (NAPLs), or both water and NAPLs are used at the same time. Vegetable oil, e.g. soybean oil, is a common choice since it is cheap, readily available, dyeable, nonaggressive and nontoxic (Hunter 2001; Jung et al. 2006). Mineral oil derivatives such as crude oil, engine oil, jet fuel, diesel and toluene have also been used (e.g. Gupta et al. 2019; Pokrajac and Deletic 2006; Wipfler et al. 2004; Zuo et al. 2021), as well as common contaminants such as trichloroethene (Fagerlund et al. 2007). Such NAPLs have to be treated with caution, as some of them can dissolve or permeate plastic tubes and seals, which can lead to spills. Therefore, such experiments need extra attention and special precaution, e.g. placing all equipment in spill tubs, keeping absorbents available and performing pre-tests with all materials intended to be in contact with the oils. Cleaning and disposal of the sand and all other oil-contaminated materials is considerably difficult. After the experiment, NAPL fluids must be disposed in a proper way, following the prevailing environmental regulations.

## Fluid control: flow and head boundaries

Most sand tank experiments study the flow of groundwater through the porous matrix from one location to another. Flow is commonly initiated by imposing a hydraulic gradient across the sand tank. The easiest and most common way of its implementation is by using two reservoirs, one at each side of the tank, which are often an integral part of the sand tank itself (example see Fig. 3). Maintaining different water levels, i.e. hydraulic heads, in the two reservoirs will induce flow.

The hydraulic connection between the reservoir and the sand can be achieved by a perforated steel plate or mesh (Fig. 3) that can be inserted through a milled groove in the inner reservoir wall, or be fixed by metal holders; however, the mesh needs to be fine enough to retain sand but coarse enough as to not impede water flow. This set-up is used to simulate a simplified vertical boundary condition, whereby the side reservoirs can be subdivided vertically into several compartments by installing sealed horizontal dividers at certain depths, e.g. when an inflow of different colors at different depths is wanted. It is also possible to supply

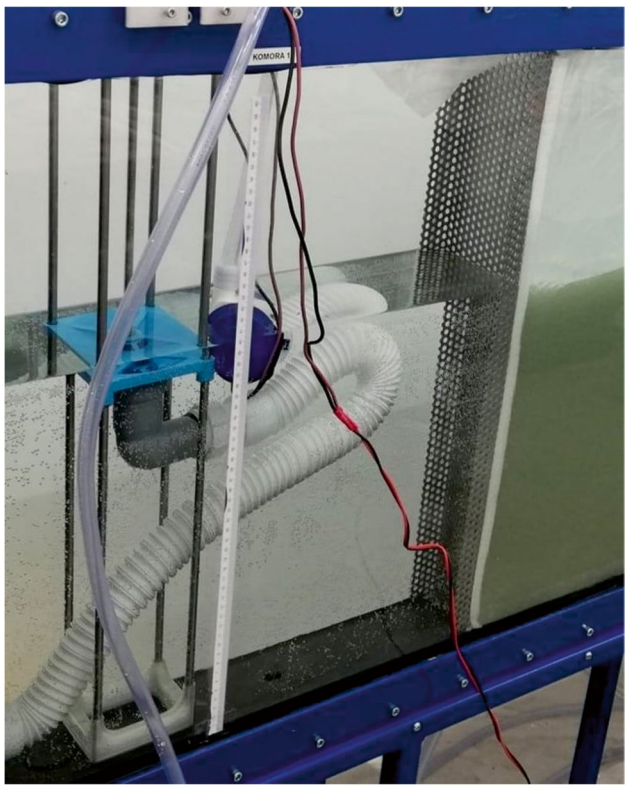


**Fig. 3** Side water reservoir (left) separated from the main chamber of the sand tank (right) by a vertical perforated steel sheet. Water level in the side water reservoir can be controlled by height adjustment of the overflow system (light blue) with its outlet hose (white). A meter scale placed at the front allows reading off the water level (here at 40 cm above bottom; Brkić and Srzić 2021)

water through individual ports at the sidewalls of the tank, each connected to separate supply reservoirs (Werner and Simmons 2009).

Depending on the research question, a head boundary may be replaced by a constant flow boundary condition; therefore, an external water reservoir is necessary, from which water is supplied to the model via tubes at defined flow rates. The volume of a sand tank reservoir itself is usually too small to maintain a constant water level and therefore has to be resupplied (or emptied) constantly from the outside. It is thus recommended to use additional external storage bottles which can store and provide enough water with a certain salinity, temperature, or color for the entire duration of the experiment.

The water levels in the reservoirs, and thus the gradient, can be controlled by overflows, where excess water spills into and then subsequently removed by pumps or tubes. Figure 3 shows an example of an overflow, adjustable in height. Another, somewhat simpler option to control the water level is a beaker or cup (without the outlet hose shown in Fig. 3), into which the water overflows. The cup has to be emptied continuously, e.g. by pumping with a peristaltic pump from above. Such a contraption was, e.g. used by the authors to remove freshwater discharging into the model ocean, which otherwise would have lead to an accumulation on top of the ocean water (Houben et al. 2018). When using hydrophobic (plastic) materials "water bridges" may form due to its surface tension, which will rupture after some time, possibly leading to small but undesired water level fluctuations in the reservoir. Alternative constructions are, e.g. pumps or siphons; however, they are usually more difficult to set up and to control.

Inflow from one of the side reservoirs (directly or via individual supply bottles) and outflow from the other allows emulating a constant head (or flux) boundary condition. It also provides a generally horizontal flow pattern, which can be useful when such conditions are prescribed by the mathematical model to be tested, e.g. if based on the Dupuit-Forchheimer assumptions. However, if recharge processes are the focus of attention, water should be supplied from the top. Water supplied from the top initially flows (mostly) vertically and then follows the general horizontal flow field (example see Fig. 1). When an unsaturated zone is present in an experiment, the unavoidable phenomenon of capillary rise has to be considered. Finer materials with smaller pore-spaces cause greater capillary rise heights, which are usually in the range of cm to dm for commonly used sands. Sediments in nature have comparable capillary rise heights, in a laboratory-scale sand tank experiment the capillary rise is thus proportionally much larger compared to the field aquifer due to the scale effect.

To the authors' understanding, the best choice for the simulation of recharge is a series of (single or paired) drippers, which are connected to a supply pump via small flexible tubes. Individual drippers provide the additional advantage of allowing individual colors to be applied for the visualization of flow paths (Fig. 1). Implementing unevenly distributed recharge rates is also possible (e.g. Dose et al. 2014; Stoeckl et al. 2015). The height of the drippers above the sand surface should not be too high to prevent splashing and the formation of impact craters. The number of drippers needs to be considered carefully, since with only a few of them, recharge might be too localized, thus not homogeneous. A large number of drippers, on the other hand, is more difficult to install and maintain as more hardware is needed. Stoeckl and Houben (2012) used 15 single drippers for an island width of 0.8 m with a spacing of 5 cm between them (Fig. 1). Houben et al. (2018) used eight pairs of drippers for an irrigated length of 0.48 m with the same spacing. In order to keep a higher number of drippers in place, it is recommended to fix them into a template, e.g. a plastic or wooden board with drilled holes. Supply from the top can also be achieved by installing a leaky reservoir tank or placing a porous tube onto the sand surface, the latter of the type used in garden irrigation. They are, however, a bit problematic, since the outflow can be quite unevenly distributed over their length.

For many experiments and their subsequent mathematical models, it is imperative to have a clear knowledge of the volume fluxes involved. Simply connecting the sand tank to the tap water supply and regulating the flow via the faucet is thus rarely an option. Peristaltic pumps have shown good potential here, both for general water supply (e.g. recharge) and pumping from model wells (Fig. 4). Most peristaltic pump models can handle one or more cassettes with several tubes each (multichannel), which is especially convenient for supply to several drippers and for the use of multiple colors at the same time (Fig. 1). The use of T- or Y-connectors for flow splitting is also possible. Flow rates of individual tubes have to be determined in any case, as small obstructions may lead to significantly different flow rates. Equal flow rates have to be ensured and should be measured individually beforehand. It should be noted that the peristaltic pump cassettes require short special tubes (the different types are color-coded), which can be connected to standard supply tubes. With longer experiments, due to the constant kneading action of the rollers, the plastic tubes can wear out and lose their flexibility or even break, and thus need to be exchanged after a couple of days. It is therefore important to also measure pumping rates from time to time during the experiment to ensure consistency. The flow rate can be adjusted in very small steps by varying the rotation speed of the pump rollers. According to the authors' experience, good pump models show a highly linear performance, thus doubling the rotation velocity doubles the outflow. It is recommended to obtain a calibration curve prior to the

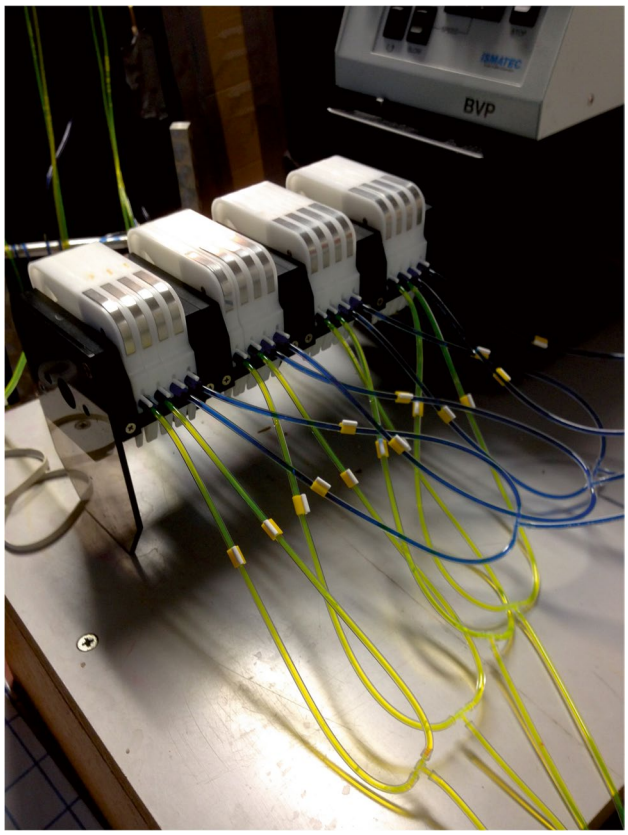


**Fig. 4** Peristaltic pump with four cassettes of four tubes each, supplying water of two different colors to drippers (please note the T-connectors)

experiment, as the pump only measures revolutions per time and not flow rates.

Another option to supply a constant rate of flow is a Mariotte bottle. It consists of a stoppered reservoir bottle, equipped with an air inlet tube and a siphon that discharges the water to the outside. The pressure at the bottom of the inlet tube (inside the bottle) remains equal to the pressure outside the bottle, which is the atmospheric pressure. The bottle thus always delivers water under constant head conditions (atmospheric pressure), regardless of the changing water level within. It should be noted that these bottles have to remain closed and cannot be resupplied during operation, thus limiting the available volume. Mariotte bottles can be easily put together from standard and cheap laboratory material; the main challenge is to get stoppers and seals airtight (Fig. 5). They have been commonly used in sand tank experiments, e.g. by Werner et al. (2009), who used 20-L bottles with 10-mm-diameter tubing connected to different ports of the model (see Fig. 6). In order to eliminate head differences between the individual bottles, they can be placed together onto height-adjustable shelves (Fig. 7) and interconnected via both the water and air components. Static sand tank experiments without hydraulic gradient are also possible, e.g. if molecular diffusion or thermal convection are the processes to be investigated.

**Fig. 5** Low-cost custom-made 2-L acrylic-glass Mariotte bottle with rubber seal at the top, ventilation pipe for maintaining constant pressure at different water levels, and a metal tube-connector outlet at the bottom. The height of this bottle is 35 cm

## Visualization using tracer dyes

The use of colored water to visualize flow paths in physical model experiments is basically as old as the use of sand tanks themselves. Adolf Thiem, a forefather of hydrogeology, used this approach already in the late 1870s to visualize flow (without density effects) towards a well screen (Houben and Batelaan 2021). Ink and unspecified dyes were often used. Another common technique was burying small crystals of potassium permanganate in the sediment, with some spacing between them, whereby water flowing past

**Fig. 6** Empty glass sand tank with steel framing and diagonal supports (sand tank dimensions are: 117.8 cm length, 120.0 cm height and 5.3 cm width). Equally spaced ports at the rear of the model are blue and in-/outlet connector valves at the sides and bottom to the (for example) Mariotte bottles are white (Werner et al. 2009)

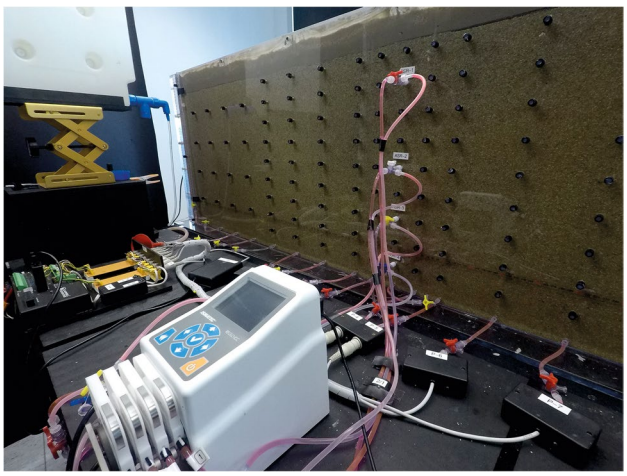

**Fig. 7** Peristaltic pump (with four cassettes, white) extracting water from four sampling ports (black) at the back of the model—emulating pumping and injection from a multi-level well, for details see Witt et al. (2021). Little black boxes in front of the tank are switches that control pumping from and injection into the ports at the bottom of the tank. Note the height-adjustable shelf for the water supply tank (white) in the background, top left corner. Total sand tank height is 0.546 m

would dissolve some of it, creating a bright purple plume in its wake. The permanganate becomes exhausted after some time and leaves a hole. Permanganate is a potent oxidizing agent, wherewith the reaction product, manganese dioxide, leaves brown stains which are difficult to remove. The technique was still used in the 1950s but has fallen out of use since (Houben and Batelaan 2021).

The most common use of colors in SWI sand tanks is the distinction between saline and freshwater and, thus, the visualization of the interface. Often the saline water is given a striking color (e.g. red) and the freshwater is left uncolored. If color tracers are injected continuously over a limited space of the infiltration area, colored flow paths will develop (Fig. 1), which can be used to visualize and quantify transport processes and travel times (e.g. Dose et al. 2014; Stoeckl and Houben 2012; Stoeckl et al. 2015). Travel times were tracked by changing the color of a steady-state flow path over time (e.g. a sequence of blue-red-blue). This results in a red parcel of colored water moving through the flow path, sandwiched between two blue parts (GeoChannel 2014). Another approach to tracing flow velocities, and also dispersion/dilution, is the release of a small volume (a few ml) of intensely colored water (tracer slug) with the same density as the surrounding water at a small injection spot over a short time. The tracer slug is injected, e.g. with a syringe through a little hole in the sand tank wall, sealed with silicone, or a previously installed port, a technique that has successfully been used to track the circulation of water in the saltwater wedge and in the freshwater part (Chang and Clement 2013; Stoeckl and Houben 2012). Stoeckl and Houben (2012) introduced a new application of colors, by changing the color of the water recharged from above at regular time intervals and different spacings (e.g. red-blue-yellow-red), which resulted in a visualization of the age stratification.

The concentration of dissolved color tracers must be small enough so that effects on density and viscosity of the fluid can be neglected. Color tracers should be conservative so that reactions with the aquifer material are negligible. Adsorption to the matrix, for example, would retard the tracer movement and result in erroneous velocity measurements and delayed breakthrough curves. Typical tracer dyes are rhodamine, uranine and eosine as well as commercial food colors (cf. Table 1). Rhodamine-WT has been identified as nonconservative in this context (Jakovovic et al. 2011; Mehdizadeh et al. 2020, 2014; Sabatini and Austin 1991), with a retardation factor of 1.3 (Jakovovic et al. 2011). Further, the application of Rhodamine-WT is not recommended anymore due to its toxicity (Leibundgut et al. 2009), especially as alternatives are available. The food dye used by Lu et al. (2013) showed no adsorption onto glass beads but slight adsorption with natural coastal sands. If adsorption is suspected, using an additional conservative tracer, such

**Table 1** Overview of color tracers used in sand tank experiments, mostly from density-dependent experiments. *ft* fluorescent tracer, *fc* food color

| Tracer | Type | Color | Concentration range [g/L] | Comments | References |
|---|---|---|---|---|---|
| Uranine | ft | Yellow | 0.3; 0.475; 0.3 | - | Rotz and Milewski (2019); Sheng et al. (2021); Stoeckl and Houben (2012) |
| Eosine | ft | Red | 0.3 | - | Stoeckl and Houben (2012) |
| Rhodamine-WT | ft | Red | 0.5–10 (500 for adsorption test) | Adsorption to matrix possible, toxic | Jakovovic et al. (2011); Mehdizadeh et al. (2014); Moore et al. (2021); Schincariol and Schwartz (1990); Werner et al. (2009) |
| Rhodamine B | ft | Red | Not specified; 0.5 | Slight adsorption | Mehdizadeh et al. (2020); Shi et al. (2011) |
| Indigotine | fc | Blue | 0.3 | Particle tracer | Stoeckl and Houben (2012) |
| New Coccine Acid Red | fc | Red | - | - | Luyun et al. (2009) |
| Brilliant Blue 2 | fc | Blue | 0.017 | - | Luyun et al. (2011) |
| Allura-Red | fc | Red | 0.15 | - | Etsias et al. (2020) |
| Dyetex Dyes Craft Colour | fc | Red | Not specified | Slight adsorption onto natural sediment | Lu et al. (2013) |
| Food color (not specified) | fc | Green | 4 | For tracer slug | Chang and Clement (2013) |
| Food color (not specified) | fc | Red | 0.5–1.0 | - | Abdoulhalik et al. (2017); Abdoulhalik and Ahmed (2018); Armanuos et al. (2019); Chang and Clement (2013); Shen et al. (2020) |
| Food color (McCormick Inc.) | fc | Red | 0.1 ml/L | - | Memari et al. (2020) |
| Organic dye in glycerine base | ? | Green | Not specified | - | Cahill (1967) |

as the electrical conductivity, is recommended as a control (Jakovovic et al. 2011). Staining of the sand tank walls must also be avoided and pre-tests for material compatibility are recommended.

Several commonly used tracers, such as uranine, eosine and rhodamine, have fluorescent properties, which allow their analytical detection even at concentrations far below the visible range. This property is often important for field tracer tests but plays a minor role in sand tank experiments where these tracers usually serve as colorants in the visible range. Another important tracer group are commercial food dyes, which are cheap, readily available in supermarkets and pose no environmental hazard when disposed. Due to their chemical composition, they can induce microbial growth and thus biofouling in the tank or reservoirs. Because of the relatively short time spans of sand tank experiments and the low concentrations used, this has not been reported as a problem so far.

Some authors have successfully used tracers that change colors to investigate mixing processes, especially at the saltwater–freshwater interface. Abarca and Clement (2009) investigated the position and thickness of the mixing zone using an indicator that changes color with different pH. They used alkaline freshwater (pH 11.6) and acidic saline water (pH 4.7), both colorless. Sodium hydroxide and hydrochloric acid were used to adapt the pH, respectively. The color indicator phenolphthalein, which changes from colorless to pink between pH 8.2 and 10, was added to the saltwater (10 ml of a 1% solution). Phenolphthalein is insensitive to salinity effects.

A similar approach was developed by de Vriendt (2021) to investigate the mixing zone. They used a chemiluminescent reaction based on luminol, which is activated by oxidation. They used two solutions, which start to directly emit light when mixed. The first solution, dissolved in the saline water, contains luminol and cobalt(II) chloride, the latter intended to enhance the oxidation. The second contains the strong oxidizing agent hydrogen peroxide, dissolved in freshwater. Under concentrations of up to 35 g/L, NaCl the reaction is insensitive to salinity effects.

Particle tracers, i.e. suspended solid particles, can also be used to track the velocity field in experiments (Jain et al. 2002). Their movement is tracked in order to visualize flow paths via particle image velocimetry. The flow field is obtained from comparing a sequence of images. The particles can be air-filled glass beads or polyamide plastic spheres and commonly have diameters between 0.5 and 50 µm. Different particle densities are available, which can be adjusted to the fluid density. Applications in coastal hydrogeology are not documented so far according to the authors'

knowledge, since the pore spaces in sands are quite small, leading to particle trapping, even for nanoparticle tracers (e.g. Li et al. 2016).

## Execution and interpretation

### Planning and scaling

As for any other scientific experiment, the execution of a sand tank experiment must be carefully planned. The duration of an experiment depends on the size of the tank and the flow rates and thus flow velocity, but moreover on the research question. Additional to the acquisition and installation of the required hardware, e.g. leveling of the experimental tank, backfilling of the porous media, preparation of sufficient amounts of different fluids, and the installation of tubes, pumps, measurement devices and auxiliary materials, certain preconditions must be thought of to ensure reliable and consistent results. A pretest can be useful to ensure the correct functioning of all components, e.g. to test for leak tightness and pump performance.

The first step is usually to establish a steady-state condition or, in the case of transient boundary conditions, a quasi steady-state, as the starting condition for the actual experiment. Times for matrix saturation and the establishment of an equilibrium may, alone, take a whole working day. Experiments may be run for several hours or days (Morgan et al. 2013), to weeks or even months (Panteleit et al. 2011), e.g. for chemical reactions considered in the latter case. Sometimes a series of consecutive experiments, including changes in, e.g. flux rates or tidal signals, is performed. In this case, it is important that the previous experiment has come to a complete stop, e.g. by having attained a hydraulic equilibrium. Switching from one transient, incomplete phase to the next can result in effects from the previous phase affecting the next one. When executing experiments for a longer time, e.g. for several days or during the night, backup systems and precautions in the case of failure must be considered. Electric devices should be placed higher than bottom level in case of water leakage to prevent electrical short-circuits or even electrocution. Worn-out peristaltic tubes should be replaced, as they affect the flow rate and may start leaking. Depending on the runtime and pump speed, tubes may have to be exchanged even during an experiment. Backup measures are always useful, e.g. when water removal pumps fail, spillways to a sink should be provided to prevent damage by inundation.

Interpretation of results must subsequently be put into the context of real-world problems. It should be noted, however, that sand tank results are not directly scalable and transferable to a (3D) field-scale environment. Sand tank experiments are small-scale models of real-world settings, and the transferability of the findings from the laboratory to the natural scale has to be studied. It is therefore important to consider the hydraulic similarity of a problem. Three types of similarity exist (Hamill 2001)—the similarity of shape (geometric similarity: e.g. beach slope or subsurface dam height); the similarity of forces (dynamic similarity: e.g. hydraulic heads at a certain location or density contrast between fresh- and saltwater); and the similarity of motion (kinematic similarity: e.g. flow velocity or direction at a specific point in time and space).

Dynamic and kinematic similarities in sand tank experiments, including variable-density flow in coastal hydrogeology, are complex and not easy to scale. The transfer of time- and space-dependent results in a laboratory experiment must be analyzed when applied to the real-world scale. Sand tank experiments on groundwater rather serve to investigate qualitative flow processes and effects of parameter changes on the results, but do not claim quantitative accuracy in real-world settings such as, e.g. hydraulic models in engineering open channel flow and sediment transport. They can, however, provide insights about hydraulic processes in certain flow systems or be used for the benchmarking of analytical and numerical model codes, which may rely on rather abstract set-ups.

### Visual recordings

It is recommended to check recording devices before every experiment to prevent data loss. The preparation time and cost for sand tank experiment can be substantial, thus checking the storage capacities of, e.g. data loggers, and the energy status of batteries and power supplies is mandatory. Recorded data of, e.g. pressure, salinity, temperature, have to be post-processed, and, e.g. plotted in graphs or time series for visualization and interpretation. Recorded images may manually or automatically be evaluated after executing an experiment.

In 2D experiments, fluid flow is mostly visualized with different tracer colors and can be directly observed from the front side of a transparent tank (sometimes also from both sides). Measurement devices, sampling ports, etc. should be installed at the rear of a tank, which leaves an unobstructed view of the front side (see auxiliary equipment). For interpretation, analysis and later presentations, images should be recorded in defined intervals throughout the experiment. Continuous video recordings produce large data files which have to be recorded, stored, and processed. If, e.g. waterproof action cameras with wide angles are used, image distortion must be taken into account and corrected. In general, it is recommended to use time-lapse photography at defined intervals (e.g. 10 s to 1 min, or even longer). If necessary, time-lapse videos can easily be produced afterwards from the single frames, and selected frames can directly be used

for publications. A continuous power supply of the digital camera has to be ensured. A reasonably big data storage medium will allow for sufficient recording time, depending on the image size and resolution. For educational purposes, videos may be a better choice than stills (e.g. GeoChannel 2014).

The selected image may cover the whole sand tank or a smaller area of interest. For visualization purposes, it should be ensured that the background is uniform and homogeneous (e.g. use a black blanket or cloth). Moreover, reflections from the surface of the tank, different light sources and colorful bright objects in the vicinity of the experiment are undesirable artifacts (Schincariol et al. 1993). Reflections are often visible in scientific publications, as they are not easy to prevent. Changing the distance or angle of the camera or light source might improve the situation. A particular useful technique is the use of light diffusers for the light sources. Reflecting objects in the room should be removed or covered. If the room or laboratory has windows, curtains should be closed during the entire experiment and artificial light sources should be used, thus ensuring consistent lighting during the recording, e.g. avoiding variations between sunny and cloudy conditions and day and night time. Direct sunlight might also lead to warming of the air temperature, which should be (1) recorded during the experiment and (2) kept as constant as possible to ensure that water temperature and thus water viscosities and densities remain constant as well.

## Automated image processing

Two-dimensional concentration distributions can be obtained by image processing techniques. This approach has the advantage that concentration distributions can be automatically obtained for successive photos. Optical imaging has a general advantage over electrical conductivity measurements, which require either the installation of several salinity probes within the sand, or on water samples taken from the tank during the experiments (the former obstruct water flow and the latter may influence the mass balance).

Methods for image recording range from binary images (Schincariol and Schwartz 1990) and the application of gray cards to determine the white balance for a more detailed distribution (Schincariol et al. 1993) to more sophisticated methods are described in the following.

Konz et al. (2008) applied an image analysis procedure using a standard reflective light technique (no transmissive light technique) and compared their data to resistivity measurement cells at the rear wall of their sand tank. They found that both lens flare effects and image resolution were a major source of error for the photometric determination of concentration, whereby attaching a light diffusor minimized the lens flare. The major perturbations of the resistivity measurement are temperature changes, which can be avoided in laboratory experiments. The main drawback of the resistivity method, however, is the unknown measurement volume of the probe. Konz et al. (2009) investigated the differences between reflective and transmissive light techniques on the salinity distribution, wherein they concluded that the reflective light technique provided fewer errors for their sand tank, which had a thickness of 4 cm. With the transmissive technique, dispersion of light travelling through the porous media occurred, consequently increasing the error. Goswami et al. (2009) distinguish between the calibration-relationship error (CRE), caused by a lack of a priori knowledge of the structure of the concentration-intensity relationship and the experimental error (EE), associated with, e.g. nonuniform lighting or other image capturing and processing issues. They proposed a statistics-based approach to evaluate the errors associated with image analysis techniques and demonstrated its robustness by analyzing a theoretical test problem. Robinson et al. (2015) applied automated image analysis to their experiments quantifying the extent of the freshwater–saltwater interface of a saltwater wedge. They performed error analysis to determine the optimum methodology for the conversion of light intensity to salinity concentration and showed that defining a relationship on a pixel-wise basis provided the most accurate method. The method was tested for glass beads of different grain sizes and tested for both steady-state and transient conditions (Robinson et al. 2016). The accuracy of the method allowed quantifying the width of the freshwater saltwater mixing zone, which is thin and rather difficult to resolve with classical visual observations. Uncertainties from image processing and analysis in sand tank DNAPL release studies were also evaluated by using reflective optical imaging on natural sand, glass beads and filtering glass (Engelmann et al. 2019).

Geoelectrical measurements from the sand surface (top) are another tool to visualize fresh- and saltwater distribution, when calibrated correctly. With the help of electrical resistivity tomography, the different electrical resistivities of fresh- and saltwater lead to different electric signals in either surface or buried electrodes. These signals can be used to calculate a 2D or 3D concentration distribution inside a sand tank, as done by, e.g. Ronczka et al. (2014). Special observation and imaging techniques are necessary for 3D experiments. Nuclear magnetic resonance imaging (NMRI), requiring a special target tracer, can be used to obtain data from the inside of a tank. Saltwater-freshwater fingering in porous media was successfully visualized in a small sand tank placed in a NMRI facility (Pearl et al. 1993). High-density water was prepared by dissolving NaCI in a solution doped with $5 \times 10^{-3}$ M nickel, to provide intensity contrast between the two solutions for imaging. When applying a magnetic field of 4.7 Tesla, the signal brightness in the images was a linear function of the

local nickel concentration. The NMRI method was also applied by Oswald et al. (2002) using dissolved copper as NMRI tracer in their 3D saltpool benchmark experiment.

### Problems and maintenance

When exposed to light for an extended period of time (often weeks), sand tanks containing wet backfill material tend to suffer from the growth of biofilms (mostly algae), which can clog the pores. Its removal is quite difficult; in the worst case the backfill material has to be exchanged completely. Chemical removal of biofilms requires aggressive chemicals, which usually contain a chlorine component or hydrogen peroxide. They are readily available from the camping and swimming pool sections of hardware stores. Maximum concentrations recommended by the supplier should not be exceeded in order to prevent damage to the sand tank and occupational health problems (e.g. through chlorine gas release). Cleaning should thus be done outside or in a well-ventilated room. Prior to its application in the sand tank, the chlorine solution should be tested for its compatibility towards the material. The easiest way to prevent algal growth is to keep the sand tank in a dark place when not in use, or to cover it with a lightproof sleeve.

The repeated backfilling of sand into the sand tank can lead to scratching of the inner surfaces, which will eventually compromise its translucence. The surfaces can be polished by using dedicated polish material for glass or acrylic-glass. Polishing inside a narrow and deep sand tank with a long handle is, however, a tedious business. It is therefore recommended to backfill and remove the sand in the most careful way, with lots of water, as described in section 'Auxiliary measurement equipment'. Metal parts in a sand tank installation can be corroded, especially when a fluid of high electrical conductivity is present, e.g. saltwater. It is therefore recommended to avoid metal if possible or to use corrosion-resistant material. Another option is the use of sacrificial anodes, e.g. made from zinc (Boufadel 2000).

The physical boundary condition (e.g. no flow at the sand tank walls) can lead to local, unintended changes in flow velocity, especially when using very coarse materials with large pores (e.g. gravel). Such grains are bounded by the walls and form large pore spaces, thus enhancing flow along the walls, which can even lead to errors, especially when wells are not placed at the center, but close to or directly at the model wall. Preventing preferential flow paths along the model walls is somehow difficult and has to be accepted. A solution would be a thin layer of transparent glue or silicone and aquifer material attached to the inner side of the sand tank walls, thus changing the surface structure.

## Outlook

The application of sand tanks for density-driven groundwater flow looks back on a long and successful history. The development of more specialized and sophisticated experiments is, however, expected for the near future—for example, the combined investigation of concentration and temperature in a single coastal aquifer experiment is a recent, new topic of interest (Nguyen et al. 2020; Pu et al. 2020, 2021). Heterogeneity is also moving more into focus, e.g. with layering but also discrete features with high or low hydraulic conductivity. Double porosity sand tank experiments are also an upcoming but still rarely investigated topic (Etsias et al. 2020). An almost unexplored field is the use of 3D printing techniques, which are becoming more common and cheaper, and could be used to print more complicated geological structures, e.g. fractured or karst aquifers but also pore structures (Ju et al. 2022).

Variable-density experiments including saltwater are an ideal test field for the investigation of new methods and arrangements in geophysical research. Direct computer tomographic observations are another upcoming technique for 3D sand tank experiments, allowing for online tracking of liquids with different densities. The technique has already been used to study the oil–water interface in porous media (e.g. Ju et al. 2022). Reactive processes are also a field with great potential for the future, e.g. the formation and expansion of fractures and caves through dissolution via mixing corrosion and its interplay with hydraulics.

It should be clear that sand tank experiments cannot be directly transferred to the field scale. An adequate representation of real-world processes by laboratory experiments can only be achieved when scaling distortions in space and time are considered—as mentioned earlier, preferential flow paths along the sand tank walls might occur. Coastal aquifers are commonly represented by natural sands (or glass beads) with relatively high hydraulic conductivities, simulating fast fluid flow, usually not taking geological heterogeneities into account. The dimensions of an experimental tank sometimes limit the representation of a coastal aquifer. Compared to the aquifer thickness, the vadose zone is often overrepresented in the experiments, due to the disproportionally thick capillary zone above the water table. Geometries are especially important when it comes to pumping—a 2D laboratory setup represents a cross-section with impermeable walls; however, pumping in the field is a 3D process, which may lead to quicker response times and/or stronger SWI or up-coning effects in the sand tank.

Despite being one of the oldest methods in coastal hydrogeology, sand tank experiments are still being done

frequently and have actually experienced some kind of renaissance over the last decade. At least in the authors' opinion, they will remain a useful tool in the future to obtain general insights into processes. Physical sand tank experiments further serve for the benchmarking of numerical model codes, and can thus not be replaced by them. A holistic review of the features and results of different sand tank experiments conducted until now would be of great interest for the community, not only for summarizing the techniques applied and results gathered so far, but also for preventing (further) duplicate experiments.

**Funding** Open Access funding enabled and organized by Projekt DEAL.

## Declarations

**Conflict of interest** The authors declare no conflict of interest.



## References

Abarca E, Clement TP (2009) A novel approach for characterizing the mixing zone of a saltwater wedge. Geophys Res Lett 36(6). https://doi.org/10.1029/2008gl036995

Abdelgawad AM, Abdoulhalik A, Ahmed AA, Moutari S, Hamill G (2018) Transient investigation of the critical abstraction rates in coastal aquifers: numerical and experimental study. Water Resour Manag 32(11):3563–3577. https://doi.org/10.1007/s11269-018-1988-3

Abdollahi-Nasab A, Boufadel MC, Li H, Weaver JW (2010) Saltwater flushing by freshwater in a laboratory beach. J Hydrol 386(1–4):1–12

Abdoulhalik A, Ahmed A, Hamill GA (2017) A new physical barrier system for seawater intrusion control. J Hydrol 549:416–427. https://doi.org/10.1016/j.jhydrol.2017.04.005

Abdoulhalik A, Ahmed AA (2018) Transience of seawater intrusion and retreat in response to incremental water-level variations. Hydrol Process 32(17):2721–2733. https://doi.org/10.1002/hyp.13214

Anwar HO (1983) The effect of a subsurface barrier on the conservation of freshwater in coastal aquifers. Water Res 17:1257–1265

Armanuos AM, Ibrahim MG, Mahmod WE, Takemura J, Yoshimura C (2019) Analysing the combined effect of barrier wall and freshwater injection countermeasures on controlling saltwater intrusion in unconfined coastal aquifer systems. Water Resour Manag 33(4):1265–1280. https://doi.org/10.1007/s11269-019-2184-9

Bear J, Dagan G (1963) Intercepting fresh water above the interface in a coastal aquifer. XIII General Assembly of the IUGG, Berkeley, CA, pp 154–181

Boluda-Botella N, Gomis-Yagües V, Ruiz-Beviá F (2008) Influence of transport parameters and chemical properties of the sediment in experiments to measure reactive transport in seawater intrusion. J Hydrol 357(1):29–41. https://doi.org/10.1016/j.jhydrol.2008.04.021

Borgman O, Darwent T, Segre E, Goehring L, Holtzman R (2019) Immiscible fluid displacement in porous media with spatially correlated particle sizes. Adv Water Resour 128:158–167. https://doi.org/10.1016/j.advwatres.2019.04.015

Boufadel MC (2000) A mechanistic study of nonlinear solute transport in a groundwater–surface water system under steady state and transient hydraulic conditions. Water Resour Res 36(9):2549–2565. https://doi.org/10.1029/2000WR900159

Brkić M, Srzić V (2021) Modeling of seawater intrusion into coastal aquifers in laboratory conditions. E-Zbornik 11:29–41. https://doi.org/10.47960/2232-9080.2021.21.11.29

Cahill JM (1967) Hydraulic sand-model study of the cyclic flow of salt water in a coastal aquifer. US Geol Surv Prof Pap 575-B:B240–B244

Cahill JM (1973) Hydraulic sand-model study of miscible-fluid flow. US Geol Surv J Res 1(2):243–250

Chang SW, Clement TP (2013) Laboratory and numerical investigation of transport processes occurring above and within a saltwater wedge. J Contam Hydrol 147:14–24. https://doi.org/10.1016/j.jconhyd.2013.02.005

Cooper CA, Glass J, Robert J, Tyler SW (2000) Double-diffusive finger convection: flow field evolution in a Hele-Shaw cell. Water Resour Res . https://www.osti.gov/biblio/772343. Accessed March 2023

de Vriendt K (2021) Mixing and chemical reaction hotspots in saline–freshwater mixing zones. PhD Thesis, Universitat Polytecnica de Catalunya, Barcelona, Spain

Dose EJ, Stoeckl L, Houben GJ, Vacher HL, Vassolo S, Dietrich J, Himmelsbach T (2014) Experiments and modeling of freshwater lenses in layered aquifers: steady state interface geometry. J Hydrol 509:621–630. https://doi.org/10.1016/j.jhydrol.2013.10.010

EN12904 (2005) Products used for treatment of water intended for human consumption: sand and gravel. European Standard. https://standards.iteh.ai/catalog/standards/cen/2d70dd7a-e717-4ed8-98db-dd6ded7e0589/en-12904-1999. Accessed March 2023

Engelmann C, Schmidt L, Werth CJ, Walther M (2019) Quantification of uncertainties from image processing and analysis in laboratory-scale DNAPL release studies evaluated by reflective optical imaging. Water 11(11):2274

Etsias G, Hamill GA, Campbell D, Straney R, Benner EM, Águila JF, McDonnell MC, Ahmed AA, Flynn R (2020) Laboratory and numerical investigation of saline intrusion in fractured coastal aquifers. Adv Water Resour 149:103866. https://doi.org/10.1016/j.advwatres.2021.103866

Fagerlund F, Illangasekare TH, Niemi A (2007) Nonaqueous-phase liquid infiltration and immobilization in heterogeneous media: 1. experimental methods and two-layered reference case. Vadose Zone J 6(3):471–482. https://doi.org/10.2136/vzj2006.0171

Fang Y, Zheng T, Zheng X, Yang H, Wang H, Walther M (2021) Influence of tide-induced unstable flow on seawater intrusion and submarine groundwater discharge. Water Resour Res 57(4):e2020WR029038. https://doi.org/10.1029/2020WR029038

Faulkner J, Hu BX, Kish S, Hua F (2009) Laboratory analog and numerical study of groundwater flow and solute transport in a karst aquifer with conduit and matrix domains. J Contam Hydrol 110(1):34–44. https://doi.org/10.1016/j.jconhyd.2009.08.004

Forchheimer P (1914) Hydraulik [Hydraulics]. Teubner, Leipzig, Germany
GeoChannel (2014) https://www.youtube.com/watch?v=1N4Fd4SxHR4. GeoChannel BGR LBEG, Hannover, Germany
Goswami RR, Ambale B, Clement TP (2009) Estimating errors in concentration measurements obtained from image analysis. Vadose Zone J 8(1):108. https://doi.org/10.2136/vzj2008.0074
Goswami RR, Clement TP (2007) Laboratory-scale investigation of saltwater intrusion dynamics. Water Resour Res 43(4):W04418
Gupta PK, Yadav B, Yadav BK (2019) Assessment of LNAPL in subsurface under fluctuating groundwater table using 2D sand tank experiments. J Environ Eng 145(9):04019048. https://doi.org/10.1061/(ASCE)EE.1943-7870.0001560
Hamill L (2001) Understanding hydraulics. Palgrave, London
Houben GJ, Batelaan O (2021) The Thiem team: Adolf and Günther Thiem, two forefathers of hydrogeology. Hydrol Earth Syst Sci Discuss 2021:1–62. https://doi.org/10.5194/hess-2021-427
Houben GJ, Stoeckl L, Mariner KE, Choudhury AS (2018) The influence of heterogeneity on coastal groundwater flow: physical and numerical modeling of fringing reefs, dykes and structured conductivity fields. Adv Water Resour 113:155–166. https://doi.org/10.1016/j.advwatres.2017.11.024
Hunter WJ (2001) Use of vegetable oil in a pilot-scale denitrifying barrier. J Contam Hydrol 53(1–2):119–131. https://doi.org/10.1016/s0169-7722(01)00137-1
Iskander M (2010) Modelling with transparent soils. Springer, Berlin
Jain N, Ottino JM, Lueptow RM (2002) An experimental study of the flowing granular layer in a rotating tumbler. Phys Fluids 14(2):572–582. https://doi.org/10.1063/1.1431244
Jakovovic D, Werner AD, Simmons CT (2011) Numerical modelling of saltwater up-coning: comparison with experimental laboratory observations. J Hydrol 402(3–4):261–273. https://doi.org/10.1016/j.jhydrol.2011.03.021
Jazayeri A, Werner AD, Wu H, Lu C (2021) Effects of river partial penetration on the occurrence of riparian freshwater lenses: experimental investigation. Water Resour Res 57(11):e2021WR029728. https://doi.org/10.1029/2021WR029728
Ju Y, Xi C, Zheng J, Gong W, Wu J, Wang S, Mao L (2022) Study on three-dimensional immiscible water–oil two-phase displacement and trapping in deformed pore structures subjected to varying geostress via in situ computed tomography scanning and additively printed models. Int J Eng Sci 171:103615. https://doi.org/10.1016/j.ijengsci.2021.103615
Jung Y, Coulibaly KM, Borden RC (2006) Transport of edible oil emulsions in clayey sands: 3D sandbox results and model validation. J Hydrol Eng 11(3):238–244. https://doi.org/10.1061/(ASCE)1084-0699(2006)11:3(238)
Konz M, Ackerer P, Huggenberger P, Veit C (2009) Comparison of light transmission and reflection techniques to determine concentrations in flow tank experiments. Exp Fluids 47(1):85–93. https://doi.org/10.1007/s00348-009-0639-0
Konz M, Ackerer P, Meier E, Huggenberger P, Zechner E, Gechter D (2008) On the measurement of solute concentrations in 2-D flow tank experiments. Hydrol Earth Syst Sci 12(3):727–738. https://doi.org/10.5194/hess-12-727-2008
Kuan WK, Jin G, Xin P, Robinson C, Gibbes B, Li L (2012) Tidal influence on seawater intrusion in unconfined coastal aquifers. Water Resour Res 48(2). https://doi.org/10.1029/2011wr010678
Kuan WK, Xin P, Jin G, Robinson CE, Gibbes B, Li L (2019) Combined effect of tides and varying inland groundwater input on flow and salinity distribution in unconfined coastal aquifers. Water Resour Res 55(11):8864–8880. https://doi.org/10.1029/2018wr024492
Leibundgut C, Maloszewski P, Külls C (2009) Artificial tracers, tracers in hydrology. Wiley-Blackwell, Oxford, UK, pp 57–122. https://doi.org/10.1002/9780470747148.ch4
Li J, Rajajayavel SRC, Ghoshal S (2016) Transport of carboxymethyl cellulose-coated zerovalent iron nanoparticles in a sand tank: effects of sand grain size, nanoparticle concentration and injection velocity. Chemosphere 150:8–16. https://doi.org/10.1016/j.chemosphere.2015.12.075
Lu C, Chen Y, Zhang C, Luo J (2013) Steady-state freshwater–seawater mixing zone in stratified coastal aquifers. J Hydrol 505:24–34. https://doi.org/10.1016/j.jhydrol.2013.09.017
Luyun R Jr, Momii K, Nakagawa K (2011) Effects of recharge wells and flow barriers on seawater intrusion. Ground Water 49(2):239–249. https://doi.org/10.1111/j.1745-6584.2010.00719.x
Luyun R, Momii K, Nakagawa K (2009) Laboratory-scale saltwater behavior due to subsurface cutoff wall. J Hydrol 377(3–4):227–236. https://doi.org/10.1016/j.jhydrol.2009.08.019
Mehdizadeh SS, Ketabchi H, Ghoroqi M, Hasanzadeh AK (2020) Experimental and numerical assessment of saltwater recession in coastal aquifers by constructing check dams. J Contam Hydrol 231:103637. https://doi.org/10.1016/j.jconhyd.2020.103637
Mehdizadeh SS, Werner AD, Vafaie F, Badaruddin S (2014) Vertical leakage in sharp-interface seawater intrusion models of layered coastal aquifers. J Hydrol 519:1097–1107. https://doi.org/10.1016/j.jhydrol.2014.08.027
Memari SS, Bedekar VS, Clement TP (2020) Laboratory and numerical investigation of saltwater intrusion processes in a circular island aquifer. Water Resour Res 56(2):e2019WR025325. https://doi.org/10.1029/2019wr025325
Moore KR, Holländer HM, Woodbury AD (2021) An experimental and numerical study of evaporite mineral dissolution and density-driven flow in porous media. J Hydrol 596:125695. https://doi.org/10.1016/j.jhydrol.2020.125695
Morgan LK, Stoeckl L, Werner AD, Post VEA (2013) An assessment of seawater intrusion overshoot using physical and numerical modeling. Water Resour Res 49(10):6522–6526. https://doi.org/10.1002/wrcr.20526
Nguyen TTM, Yu X, Pu L, Xin P, Zhang C, Barry DA, Li L (2020) Effects of temperature on tidally influenced coastal unconfined aquifers. Water Resour Res 56(4):e2019WR026660. https://doi.org/10.1029/2019WR026660
Nomitsu T, Kamimoto R, Toyohara Y (1929) On the adsorption of a NaCl-solution by sand. Mem Coll Sci Kyoto Imperial Univ, Ser A, XII(5):265–274
Oliviera IB, Demond AH, Salehzadeh A (1996) Packing of sands for the production of homogeneous porous media. Soil Sci Soc Am J 60(1):49–53. https://doi.org/10.2136/sssaj1996.03615995006000010010x
Oswald SE, Scheidegger MB, Kinzelbach W (2002) Time-dependent measurement of strongly density-dependent flow in a porous medium via nuclear magnetic resonance imaging. Transp Porous Media 47(2):169–193. https://doi.org/10.1023/A:1015508410514
Oz I, Eyal S, Yoseph Y, Ittai G, Elad L, Haim G (2016) Salt dissolution and sinkhole formation: results of laboratory experiments. J Geophys Res: Earth Surf 121(10):1746–1762. https://doi.org/10.1002/2016JF003902
Panteleit B, Hamer K, Kringel R, Kessels W, Schulz HD (2011) Geochemical processes in the saltwater–freshwater transition zone: comparing results of a sand tank experiment with field data. Environ Earth Sci 62(1):77–91. https://doi.org/10.1007/s12665-010-0499-1

Pearl Z, Magaritz M, Bendel P (1993) Nuclear magnetic resonance imaging of miscible fingering in porous media. Transp Porous Media 12(2):107–123. https://doi.org/10.1007/BF00616975

Pennink JMK (1905) Grondwater stroombanen [Groundwater flow paths]. Stadsdrukkery Amsterdam. http://citg.tudelft.nl/index.php?id=19739&L=1. Accessed March 2023

Pokrajac D, Deletic A (2006) Experimental study of LNAPL migration in the vicinity of a steep groundwater table. Soils Found 46(3):271–280. https://doi.org/10.3208/sandf.46.271

Pollock D, Cirpka OA (2012) Fully coupled hydrogeophysical inversion of a laboratory salt tracer experiment monitored by electrical resistivity tomography. Water Resour Res 48(1). https://doi.org/10.1029/2011wr010779

Pool M, Dentz M, Post VEA (2016) Transient forcing effects on mixing of two fluids for a stable stratification. Water Resour Res 52(9):7178–7197. https://doi.org/10.1002/2016WR019181

Pu L, Xin P, Nguyen TTM, Yu X, Li L, Barry DA (2020) Thermal effects on flow and salinity distributions in coastal confined aquifers. Water Resour Res 56(10):e2020WR027582. https://doi.org/10.1029/2020WR027582

Pu L, Xin P, Yu X, Li L, Barry DA (2021) Temperature of artificial freshwater recharge significantly affects salinity distributions in coastal confined aquifers. Adv Water Resour 156:104020. https://doi.org/10.1016/j.advwatres.2021.104020

Robinson G, Ahmed AA, Hamill GA (2016) Experimental saltwater intrusion in coastal aquifers using automated image analysis: applications to homogeneous aquifers. J Hydrol 538:304–313. https://doi.org/10.1016/j.jhydrol.2016.04.017

Robinson G, Hamill GA, Ahmed AA (2015) Automated image analysis for experimental investigations of salt water intrusion in coastal aquifers. J Hydrol 530:350–360. https://doi.org/10.1016/j.jhydrol.2015.09.046

Ronczka M, Stoeckl L, Günther T (2014) Geoelectrical monitoring of freshwater–saltwater interaction in physical model experiments. In: Helga Wiederhold JM, Hinsby K, Nommensen B (eds) Proceedings of the 23rd Salt Water Intrusion Meeting Husum, Germany, pp 331–334

Röper T, Greskowiak J, Massmann G (2015) Instabilities of submarine groundwater discharge under tidal forcing. Limnol Oceanogr 60(1):22–28. https://doi.org/10.1002/lno.10005

Rotz RR, Milewski AM (2019) Physical modeling of inland freshwater lens formation and evolution in drylands. Hydrogeol J 27(5):1597–1610. https://doi.org/10.1007/s10040-019-01940-1

Rumer RR, Harleman DRF (1963) Intruded salt-water wedge in porous media. J Hydraul Div 89(6):193–220. https://doi.org/10.1061/JYCEAJ.0000954

Sabatini DA, Austin TA (1991) Characteristics of rhodamine WT and fluorescein as adsorbing ground-water tracers. Groundwater 29(3):341–349. https://doi.org/10.1111/j.1745-6584.1991.tb00524.x

Schincariol RA, Herderick EE, Schwartz FW (1993) On the application of image analysis to determine concentration distributions in laboratory experiments. J Contam Hydrol 12(3):197–215. https://doi.org/10.1016/0169-7722(93)90007-F

Schincariol RA, Schwartz FW (1990) An experimental investigation of variable density flow and mixing in homogeneous and heterogeneous media. Water Resour Res 26(10):2317–2329. https://doi.org/10.1029/WR026i010p02317

Sharma B, Bhattacharjya RK (2020) Behaviour of contaminant transport in unconfined coastal aquifer: an experimental evaluation. J Earth Syst Sci 129(1):140. https://doi.org/10.1007/s12040-020-01405-0

Shen Y, Xin P, Yu X (2020) Combined effect of cutoff wall and tides on groundwater flow and salinity distribution in coastal unconfined aquifers. J Hydrol 581:124444. https://doi.org/10.1016/j.jhydrol.2019.124444

Sheng C, Jiao J, Xu H, Liu Y, Luo X (2021) Influence of land reclamation on fresh groundwater lenses in oceanic islands: laboratory and numerical validation. Water Resour Res 57. https://doi.org/10.1029/2021WR030238

Shi L, Cui L, Park N, Huyakorn PS (2011) Applicability of a sharp-interface model for estimating steady-state salinity at pumping wells: validation against sand tank experiments. J Contam Hydrol 124(1–4):35–42. https://doi.org/10.1016/j.jconhyd.2011.01.005

Stoeckl L, Houben G (2012) Flow dynamics and age stratification of freshwater lenses: experiments and modeling. J Hydrol 458–459(0):9–15. https://doi.org/10.1016/j.jhydrol.2012.05.070graf

Stoeckl L, Houben GJ, Dose EJ (2015) Experiments and modeling of flow processes in freshwater lenses in layered island aquifers: analysis of age stratification, travel times and interface propagation. J Hydrol 529:159–168. https://doi.org/10.1016/j.jhydrol.2015.07.019

Stoeckl L, Walther M, Morgan LK (2019) Physical and numerical modelling of post-pumping seawater intrusion. Geofluids 2019:11. https://doi.org/10.1155/2019/7191370

Thorenz C, Kosakowski G, Kolditz O, Berkowitz B (2002) An experimental and numerical investigation of saltwater movement in coupled saturated–partially saturated systems. Water Resour Res 38(6):5-1–5-11. https://doi.org/10.1029/2001wr000364

Vats OP, Sharma B, Stamm J, Bhattacharjya RK (2020) Groundwater circulation well for controlling saltwater intrusion in coastal aquifers: numerical study with experimental validation. Water Resour Manag 34(11):3551–3563. https://doi.org/10.1007/s11269-020-02635-z

Werner AD, Jakovovic D, Simmons CT (2009) Experimental observations of saltwater up-coning. J Hydrol 373(1–2):230–241

Werner AD, Simmons CT (2009) Impact of sea-level rise on sea water intrusion in coastal aquifers. Ground Water 47(2):197–204. https://doi.org/10.1111/j.1745-6584.2008.00535.x

Wipfler EL, Ness M, Breedveld GD, Marsman A, van der Zee SEATM (2004) Infiltration and redistribution of LNAPL into unsaturated layered porous media. J Contam Hydrol 71(1):47–66. https://doi.org/10.1016/j.jconhyd.2003.09.004

Witt L, Müller MJ, Gröschke M, Post VEA (2021) Experimental observations of aquifer storage and recovery in brackish aquifers using multiple partially penetrating wells. Hydrogeol J. https://doi.org/10.1007/s10040-021-02347-7

Wooding RA, Tyler SW, White I (1997) Convection in groundwater below an evaporating salt lake: 1. onset of instability. Water Resour Res 33(6):1199–1217. https://doi.org/10.1029/96wr03533

Wu L-H, Zhuang S-Y (2010) Experimental investigation of effect of tide on coastal groundwater table. J Hydrodyn 22(1):66–72. https://doi.org/10.1016/S1001-6058(09)60029-9

Wu P, Shu L, Yang C, Xu Y, Zhang Y (2019) Simulation of groundwater flow paths under managed abstraction and recharge in an analogous sand-tank phreatic aquifer. Hydrogeol J 27(8):3025–3042. https://doi.org/10.1007/s10040-019-02029-5

Yu X, Xin P, Lu C (2019) Seawater intrusion and retreat in tidally-affected unconfined aquifers: laboratory experiments and numerical simulations. Adv Water Resour 132:103393. https://doi.org/10.1016/j.advwatres.2019.103393

Zhang Q, Volker RE, Lockington DA (2002) Experimental investigation of contaminant transport in coastal groundwater. Adv Environ Res 6(3):229–237. https://doi.org/10.1016/S1093-0191(01)00054-5

Zhang Y, He G, Wu J, Yu J, Gong X (2022) Laboratory experimental study on pumping-induced earth fissures. Hydrogeol J 30(3):849–864. https://doi.org/10.1007/s10040-022-02473-w

Zhou J, Zheng X, Flury M, Lin G (2009) Permeability changes during remediation of an aquifer affected by sea-water intrusion: a

laboratory column study. J Hydrol 376(3):557–566. https://doi.org/10.1016/j.jhydrol.2009.07.067

Zuo R, Zhao X, Yang J, Pan M, Xue Z, Gao X, Wang J, Teng Y (2021) Analysis of the LNAPL migration process in the vadose zone under two different media conditions. Int J Environ Res Public Health 18(21). https://doi.org/10.3390/ijerph182111073